Available online at www.sciencedirect.com
SCIENCE DIRECT®
Journal of Sound and Vibration 275 (2004) 1027–1050
JOURNAL OF SOUND AND VIBRATION
www.elsevier.com/locate/jsvi

Tip clearance noise of axial flow fans operating at design and off-design condition

T. Fukano*, C.-M. Jang

Department of Mechanical Science and Engineering, Kyushu University, 6-10-1, Hakozaki, Higashi-ku, Fukuoka 812-8581, Japan

Received 13 January 2003; accepted 4 July 2003

Abstract

The noise due to tip clearance (TC) flow in axial flow fans operating at a design and off-design conditions is analyzed by an experimental measurement using two hot-wire probes rotating with the fan blades. The unsteady nature of the spectra of the real-time velocities measured by two hot-wire sensors in a vortical flow region is investigated by using cross-correlation coefficient and retarded time of the two fluctuating velocities. The results show that the noise due to TC flow consists of a discrete frequency noise due to periodic velocity fluctuation and a broadband noise due to velocity fluctuation in the blade passage. The peak frequencies in a vortical flow are mainly observed below at four harmonic blade passing frequency. The discrete frequency component of velocity fluctuation at the off-design operating conditions is generated in vortical flow region as well as in reverse flow region. The peak frequency can be an important noise source when the fans are rotated with a high rotational speed. The authors propose a spiral pattern of velocity fluctuation in the vortical flow to describe the generation mechanism of the peak frequency in the vortical flow. In addition, noise increase due to TC flow at low flow rate condition is analyzed with relation to the distribution of velocity fluctuation due to the interference between the tip leakage vortex and the adjacent pressure surface of the blade.

1. Introduction

The present study is focused on the mechanism of sound generation due to unsteady behavior of vortical flow near the rotor tip in axial flow fans. The nature of a tip leakage vortex observed in a rotor tip region has been studied by many researchers because of its important role on the flow field; for example, Inoue and Kuroumaru [1], Storer and Cumpsty [2], and Lakshminarayana et al. [3].

*Corresponding author. Tel./fax: +81-926-423392.
E-mail address: fukanot@mech.kyushu-u.ac.jp (T. Fukano).

0022-460X/$ - see front matter © 2003 Elsevier Ltd. All rights reserved.
doi:10.1016/S0022-460X(03)00815-0

They showed that the tip leakage flow has a three-dimensional and an unsteady nature, and effect on a loss production and a noise generation. However, most studies are mainly focused on the vortical flow in a blade passage with relation to aerodynamic performance without considering the sound generation due to the unsteady behavior of the vortical flow.

Noise level increase by enlarging a tip clearance (TC) is studied by Longhouse [4], Fukano et al. [5], and Kameier and Neise [6]. Their studies showed that the spectral peaks occurred in sound spectra although a TC noise is broadband naturally. Kameier and Neise [6] also reported that the TC noise associated with a rotating flow instability in axial turbomachines was generated under reverse flow conditions in a TC gap. However, the above studies were performed without detailed flow analysis in the blade passage. The understanding of the detailed flow structure as well as the spectrum of a fluctuating velocity in the blade passage is important to analyze the generation mechanism of the TC noise, which is closely related to the unsteady behavior of the tip leakage vortex.

On the other hand, the measurement of the real-valued signal with a high sampling frequency in the stationary frame is nearly impossible in the blade passage of axial turbomachines. Therefore, it is essential to measure a real-time velocity in the relative frame of reference rotating with a rotor to readily understand the frequency characteristics of a fluctuating vortical flow in the rotor blade. Detailed measurements of a velocity and a velocity fluctuation in the axial flow fans are made using a rotating hot-wire sensor near the rotor tip in the rotating frame in the present study.

The pioneer study of the flow measurement in the rotational frame was performed by Fukano et al. [7]. They measured the periodic velocity fluctuation in the downstream of the trailing edge of a rotating flat-plate blade using a hot-wire sensor attached to the originally designed measuring system. The result showed the important role of the periodic velocity fluctuation due to Karman vortex street in the generation of broadband noise.

In the present study, spectra of the velocity fluctuation near rotor tip were measured using the rotating hot-wire sensor to elucidate the TC noise in the axial flow fans with relation to the distribution of the relative velocity and the velocity fluctuation. The unsteady nature of the spectra of the real-time velocities measured by two hot-wire sensors in the vortical flow region is also investigated by using cross-correlation coefficient and retarded time of the two fluctuating velocities. The present study was performed at off-design operating conditions as well as a design flow condition. In addition, the TC effects on the vortical flow field and the aerodynamic noise generation are also reviewed by introducing two different TCs to the axial flow fans.

2. Experimental apparatus and procedures

2.1. Test axial flow fan

The present study was performed on low speed axial flow fans in two cases of the TC of 2 mm (1.6 per cent tip chord) and 4.5 mm (3.5 per cent tip chord). Its design specifications for the fan having 2 mm TC are summarized in Table 1. The fan has a design flow coefficient Φ (mean axial velocity divided by rotor tip speed) of 0.39 and a design static pressure rise coefficient Ψ_S (static pressure rise divided by dynamic pressure at rotor tip) of 0.26. Fig. 1 shows the pressure rise Ψ_S and the sound pressure level SPL plotted against flow rate of the test fan. The rotor blade has

Table 1
Design specifications of axial flow fan

Flow coefficient	0.39
Pressure coefficient	0.26
Rotational speed	1000 r.p.m.
Tip radius	287.5 mm
Hub-tip ratio	0.52
Blade profile	NACA65
Number of blade	8

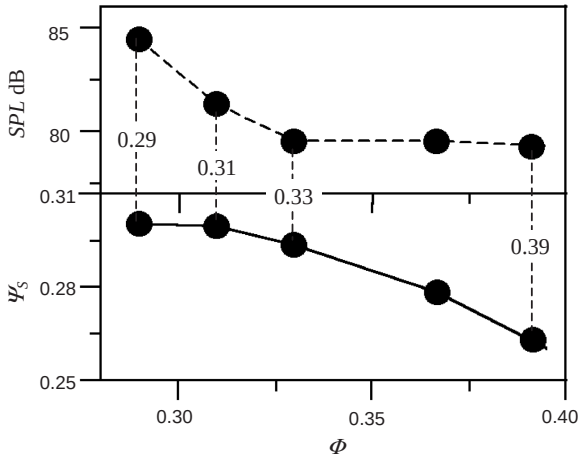

Fig. 1. Sound pressure level and static pressure rise ($TC = 2$ mm, $N = 1000$ r.p.m.).

NACA 65 series profile sections designed by free vortex operation. The blade stagger angle and the angle of attack at the rotor tip are 64.2° and 4.4°, respectively. The experimental measurements were carried out at the off-design operating conditions of $\Phi = 0.33$, 0.31 and 0.29 (25 per cent lower than the design flow rate) as well as at the design condition of $\Phi = 0.39$ while rotational speed of the fan rotor was kept constant, 1000 r.p.m. The blade tip section of the rotor has the solidity of 0.55 and the chord length of 129 mm. Reynolds number based on the rotor tip speed and the rotor tip chord length is 2.6×10^5.

The three-dimensional vortical flow structure in the axial flow fans operating at the design condition was analyzed by numerical simulation and experimental measurement in the previous study [8]. Three-dimensional tip leakage vortex structure and leakage streamlines surrounding the tip leakage vortex obtained by the numerical simulation for the axial flow fan having 2 mm TC are shown in Fig. 2, which is a perspective view from the casing side. The vortex core identification method and the definition of normalized helicity H_n were presented in detail in the previous paper [8]. It was found that the tip leakage vortex formed close to the leading edge of the blade tip on suction side grew in the streamwise direction, and formed a local recirculation region resulting from a vortex breakdown inside the blade passage as shown in Fig. 2.

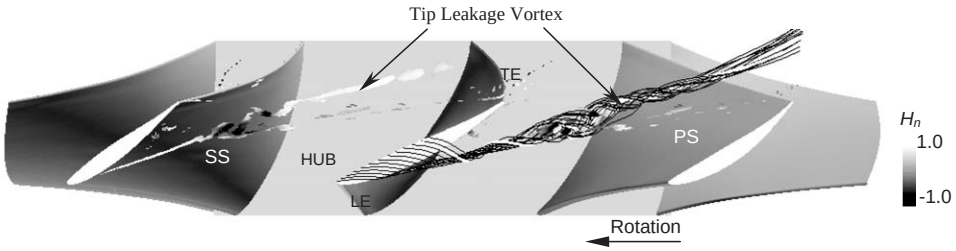

Fig. 2. Vortex cores colored with normalized helicity and leakage streamlines surrounding tip leakage vortex (black lines in right passage) near rotor tip ($TC = 2$ mm, $\Phi = 0.39$).

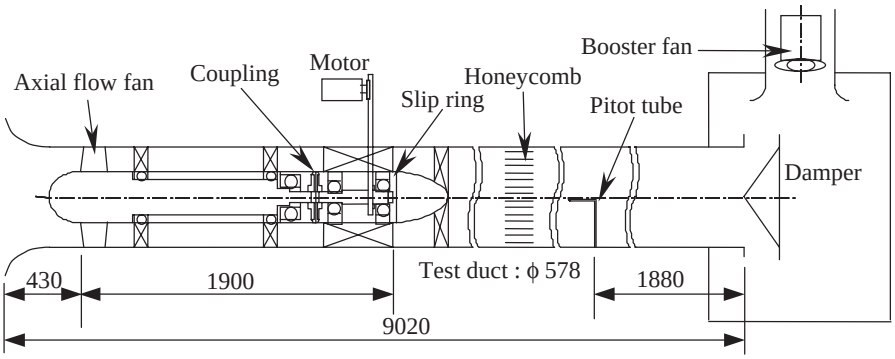

Fig. 3. Experimental set-up (units: mm).

2.2. Measuring procedures

Fig. 3 shows the experimental set-up along with its major dimensions. It was an open-loop facility having the duct inner diameter of 0.579 m. The facility consisted of a bellmouth inlet, a fan driving motor connected by the belt, a damper and a booster fan. The aerodynamically designed damper was used to adjust the flow rates. The distance between the bellmouth inlet and the test fan was 0.43 m.

A schematic view of the measuring system is shown in Fig. 4. Two hot-wire sensors rotating with the fan rotor were introduced for the present study to obtain the cross-correlation between a reference position and target (traversing) positions, as well as the three-dimensional velocity and velocity fluctuation inside and downstream of the rotor blade. The I-type sensor of the hot-wire probe was a tungsten filament wire of 5-μm diameter. The wires of the both probe sensors were set parallel to the radial direction of the rotor blade. The supporter of the fixed probe as shown in Fig. 4 was directly installed on the hub. The traversing probe was controlled by the three-dimensional traversing system, i.e., radial, axial and rotational directions, installed inside of the hub with traverse resolution of 0.3 mm. The maximum traversing span of the traversing system in radial, axial and tangential directions was 45 mm, 50 mm and 50° (45° for one blade passage), respectively. Therefore, it could measure one blade passage of the tip region without rearranging the traversing system while the rotor was in motion. The real-valued velocity fluctuations were measured by using constant-temperature hot-wire anemometer and interfacing technique with an

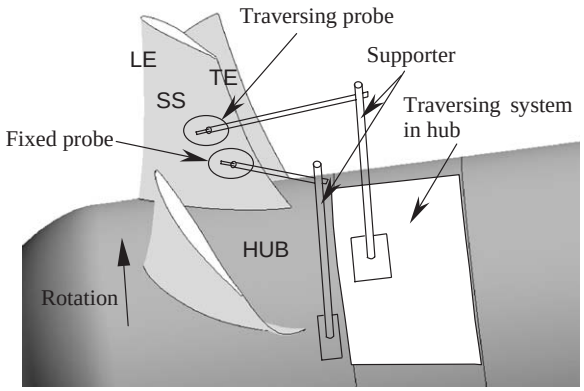

Fig. 4. Test blade and measuring system.

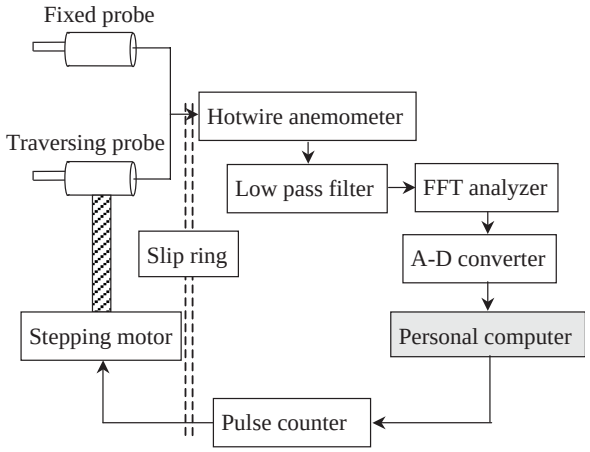

Fig. 5. Diagram of on-line system (for measuring real-valued velocity fluctuation).

on-line computer. The diagram of the on-line system is shown in Fig. 5. The output from the hot-wire probe was carried from a rotating frame to a stationary frame through Michigan Scientific Corporation mercury slip-ring unit installed inside of the hub as shown in Fig. 3. The signal obtained from the hot-wire anemometer was filtered out the frequency above 8.9 kHz using the low pass filter as shown in Fig. 5.

Three-dimensional velocity and velocity fluctuation inside and downstream of the rotor blade were measured by the traversing probe, and determined by using a constant-temperature hot-wire anemometer and averaging technique with an on-line computer. Ensemble averaged values of the velocity and the velocity fluctuation were obtained by 6000 sampling data at each measuring position. The spectrum analysis of the velocity fluctuation was performed using Onosokki FFT analyzer. The calibration of the probe at the measuring system was performed by detaching the rotor blade from the test fan and measuring the tangential velocity for the four different rotational frequencies: 300, 600, 900 and 1200 r.p.m. In addition, the magnitude of the deformation of the

probe supporter caused by the rotor rotation was calibrated prior to the experiments. The experiments with rotor blade having the TC of 2 and 4.5 mm were conducted by changing the rotor tip diameter while the inner diameter of the casing was kept constant.

On the other hand, the noise generated from the rotor blades was measured at the position of 1 m upstream from the fan rotor and on the rotational axis. In the measurement of the noise spectrum, the background noise kept 5 dB below the sound level of all frequencies. It is noted that the noise is obtained from the measuring system that only the fan rotor is excluded.

3. Results and discussion

3.1. Noise increase due to the interaction of a leakage flow and an adjacent rotor blade

As shown in Fig. 1, the sound pressure level SPL is sharply increased from the flow rate of $\Phi = 0.33$ as a flow rate is decreased. It is noted that the flow condition is not in a stall at $\Phi = 0.29$ from the pressure rise Ψ_S shown in Fig. 1. The reason why the SPL is increase at the low flow rate between $\Phi = 0.33$ and $\Phi = 0.29$ will be discussed in the following.

Fig. 6 shows the distribution of the relative velocity on the plane of 99 per cent span of the blade in the test fan having 2 mm TC for the design ($\Phi = 0.39$) and the two off-design operating conditions ($\Phi = 0.33$ and 0.29), which is a perspective view from the casing. The relative velocity V_{at} is defined and normalized by the circumferential velocity of the blade tip, U_t:

$$V_{at} = \frac{\sqrt{V_a^2 + V_t^2}}{U_t}, \tag{1}$$

where V_a and V_t denote axial velocity and tangential (circumferential) velocity, respectively. In Fig. 6, the low velocity region in the blade passage results from the tip leakage vortex as shown in Fig. 2 [8]. The tip leakage vortex formed on suction side grows in the downstream direction

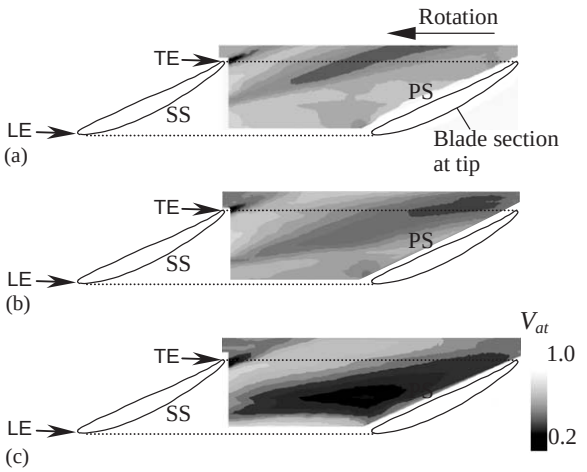

Fig. 6. Distribution of relative velocity on the plane of 99 per cent span ($TC = 2$ mm): (a) $\Phi = 0.39$, (b) $\Phi = 0.33$, and (c) $\Phi = 0.29$.

without interference with the adjacent pressure surface in the design operating condition. However, the tip downstream side of the leakage vortex is moved upstream compared to the case of the $\Phi = 0.39$ as the flow rate is decreased, thus resulting in interference with the adjacent pressure surface as shown in Fig. 6.

Fig. 7 shows the distribution of the velocity fluctuation on the plane of 99 per cent span, which is presented in the same condition as shown in Fig. 6. The velocity fluctuation V_f is defined by

$$V_f = \frac{\sqrt{\overline{V_{at}'^2}}}{U_t}, \tag{2}$$

where $\overline{V_{at}'}$ is the fluctuating component of the relative velocity defined by Eq. (1). The high velocity fluctuation on the each plane is observed near the corresponding low velocity region shown in Fig. 6. It is well known that the high velocity fluctuation is closely related to the aerodynamic noise generation. It should be noted that the high velocity fluctuation region in the blade passage is enlarged as the flow rate is decreased. The increase of the broadband noise in the low flow rate conditions is mainly caused by the high velocity fluctuation as shown in Fig. 7.

Figs. 8(a)–(c) shows the distribution of the velocity fluctuation downstream of the rotor blade having 2 mm TC for the same flow conditions shown in Figs. 6 and 7. The measuring plane, which is nearly perpendicular to streamwise direction, is located 2.7 mm downstream from the blade trailing edge. In the figure, the horizontal axis represents the perpendicular distance η to the streamwise direction from the blade trailing edge. The high velocity fluctuation near the pressure surface of the rotor tip is not observed in the design operating condition as shown in Fig. 8(a) because the tip leakage vortex is moved downstream without interference with the adjacent pressure surface as described in Fig. 6(a). However, the high velocity fluctuation region moves closer to the pressure side as the flow rate decreases, and the tip leakage vortex interferes with the pressure surface as clearly shown in Figs. 8(b) and (c). Especially, the highest velocity fluctuation presents near the pressure surface (○ in Fig. 8(c)) in the lowest flow condition ($\Phi = 0.29$). The

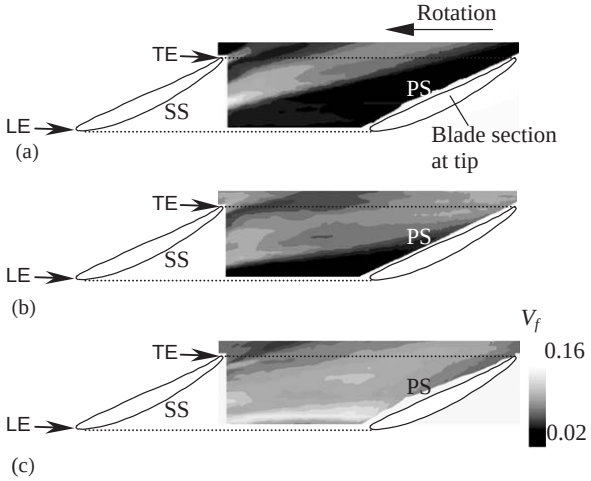

Fig. 7. Distribution of velocity fluctuation on the plane of 99 per cent span ($TC = 2$ mm): (a) $\Phi = 0.39$, (b) $\Phi = 0.33$, and (c) $\Phi = 0.29$.

high velocity fluctuation near the pressure surface induces high pressure fluctuation on the blade surface, which has strongly effect on the fan noise generation because of the dipole characteristic of the pressure fluctuation on the solid surface [9].

Fig. 9 shows the spectra of noise in the fan having 2 mm TC for the three off-design operating conditions: $\Phi = 0.29$, 0.31 and 0.33. In the figure, vertical dashed lines indicate the harmonic frequencies of blade passing where the fundamental blade passing frequency BPF is 133 Hz. The sampling frequency of the present measurement is 5012 Hz, and the frequency below 1200 Hz is

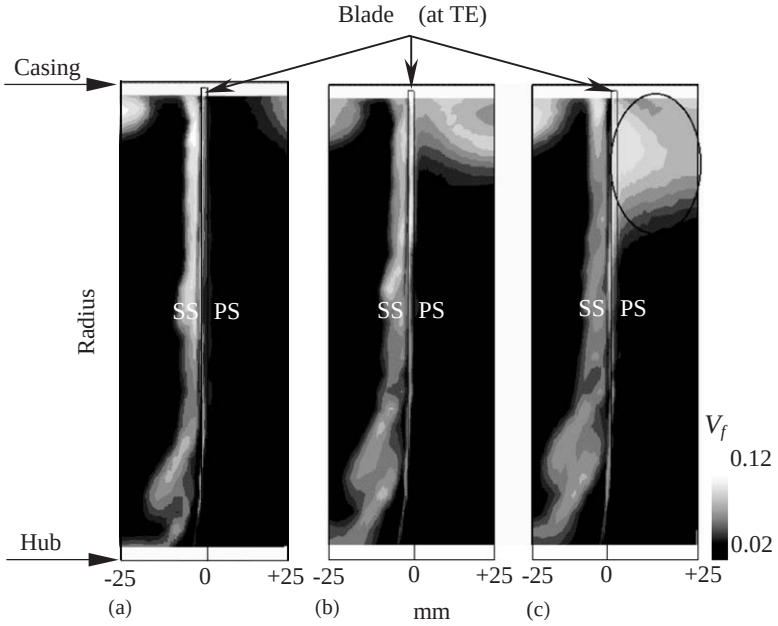

Fig. 8. Distribution of velocity fluctuation downstream of rotor blade ($TC = 2$ mm): (a) $\Phi = 0.39$, (b) $\Phi = 0.33$, and (c) $\Phi = 0.29$.

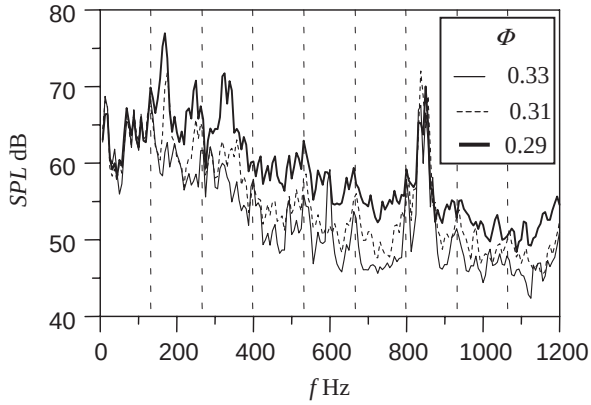

Fig. 9. Spectra of noise ($TC = 2$ mm).

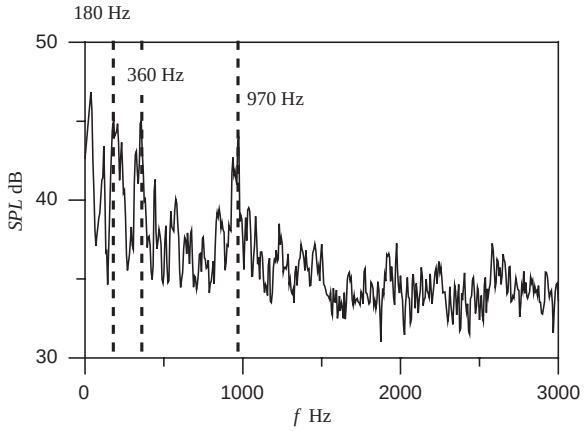

Fig. 10. Spectrum of noise in the case of a white noise source.

only presented because the sound pressure level over the 1200 Hz has almost same value irrespective of the flow rate Φ. The spectral peaks at the 840 Hz, which have almost same sound pressure level, are generated by the fan driving motor shown in Fig. 3. The noise increase below the flow rate $\Phi = 0.33$, which has a same sound pressure level of the design operating condition as shown in Fig. 1, is mainly caused by the stronger velocity fluctuation as described in the Fig. 7 which interacts with the duct inner surface and the adjacent blade. The spectral peaks at 170, 250 and 330 Hz excepting the harmonic of BPF are also observed at $\Phi = 0.29$, 0.31 and 0.33. To investigate spectral characteristics due to the duct installed downstream of the fan rotor, a speaker generating a white noise was installed 9 m downstream from the fan rotor, and spectrum of the noise was measured at the position of 1 m upstream from the fan rotor and on the rotational axis. The spectral peaks of 180, 360 and 970 Hz having a relatively wide frequency band are observed in Fig. 10. It can be considered that the high peaks at the 170 and the 330 Hz shown in Fig. 9 are influenced by frequencies caused by the duct, 180 and 360 Hz. It should be noted that the noise increase at the low flow rate condition is mainly caused by the high velocity fluctuation in the vortical flow interacting with the duct surface and the adjacent pressure surface.

We will discuss the mechanism of the generation of the discrete frequency component more in the later part of this paper.

3.2. Three-dimensional vortical flow structure

To investigate the three-dimensional structure of the vortical flow near the rotor tip, the relative velocity in the blade passage and downstream was measured by the hot-wire sensor (traversing probe in Fig. 4) rotating with rotor blade in the off-design operating condition ($\Phi = 0.31$) and in the design condition ($\Phi = 0.39$). The structure of the vortical flow was also analyzed for the two different TCs (2 and 4.5 mm) at the both operating conditions to understand the TC effect on the vortical flow.

The hot-wire sensor mounted inside of the hub was moved by the traversing system as already shown in Fig. 4. The interval of measuring positions is about 5 mm in the pitchwise direction, and

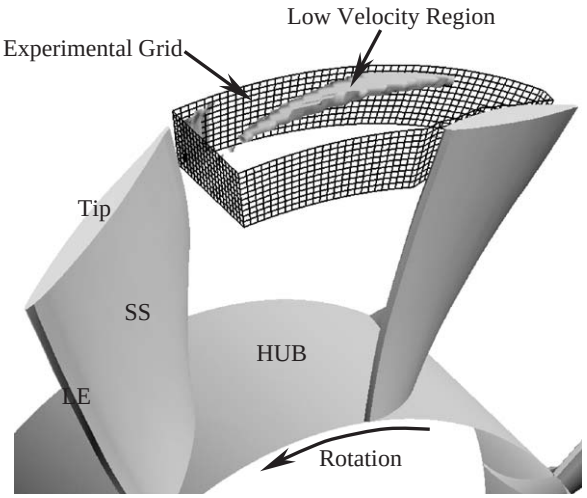

Fig. 11. Experimental grid and low velocity region ($V_{at}/U_t < 0.75$) in the design operating condition ($TC = 2$ mm).

3 mm in the streamwise direction and in the spanwise direction. The measuring area in the radial direction is from 255 mm (76 per cent span) to 280 mm (98 per cent span). Fig. 11 shows an experimental grid and a measured low velocity region in the blade passage for the fan having 2 mm TC. In the figure, the relative velocity V_{at} is normalized by the rotor tip speed U_t, and only the low relative velocity region with $V_{at}/U_t < 0.75$ is shown. The position of the leakage streamlines shown in Fig. 2, which are the result of the numerical simulation [8], correspond well to that of the low velocity region. It should be noted that the low velocity region in the blade passage is caused by the tip leakage vortex [8].

To compare the structure of the tip leakage vortex in the cases of the design and the off-design conditions, the measured low relative velocity region is reproduced in the blade passage. Fig. 12 shows the distributions of the low relative velocity with the measuring region for the 2 and the 4.5 mm TCs, which are the perspective view from the casing. The regions colored with white and black in Fig. 12 represent the low velocity area obtained in the off-design and the design operating condition, respectively. In the figure, the scale of the velocity region has a different value. The low velocity region due to the tip leakage vortex is clearly observed in the blade passage. It is found that the tip leakage vortex obtained at the off-design condition is located upstream compared to that at the design condition for the both TCs. This is generally acknowledged as described by Inoue et al. [1] in the axial compressor rotor. It can also be understood that the low velocity region spreads out as the flow rate is decreased, which is caused by the larger movement of the tip leakage vortex in this low flow rate condition. A large vortical flow is generated due to the larger leakage flow as the TC is increased. The detailed vortical flow and its comparison to the result obtained by numerical simulation in the design operating condition was performed in the previous paper [8].

3.3. Spectral peaks of fluctuating velocity at a design operating condition

To investigate the behavior of the flow fluctuation in the blade passage, distributions of the velocity fluctuation on a quasi-orthogonal plane to the tip leakage vortex at the design operating

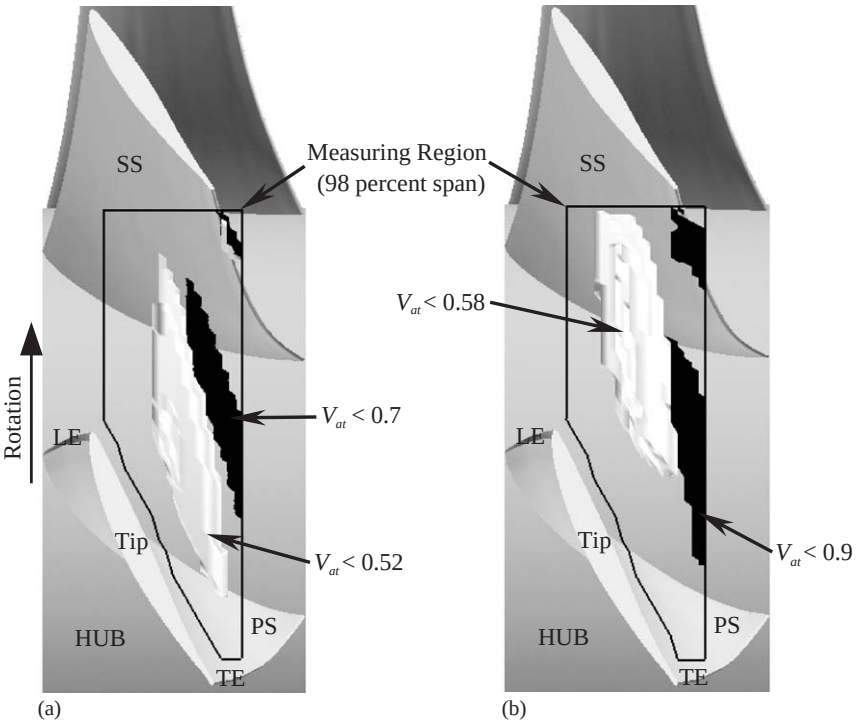

Fig. 12. Low relative velocity region in a design ($\Phi = 0.39$, black region) and an off-design operating condition ($\Phi = 0.31$, white region): (a) $TC = 2$ mm and (b) $TC = 4.5$ mm.

condition are shown in Fig. 13 with relation to the distribution of the relative velocity. The position of the quasi-orthogonal plane to the tip leakage vortex in the blade passage, which is a perspective view from casing, is shown in Fig. 13(c). In the figure, positions of A and G in the plane are located upstream and downstream of the vortex, respectively. From the distribution of the relative velocity as shown in Fig. 13(a), it can be clearly observed the vortical flow due to the tip leakage vortex. The vortical flow is formed at a low velocity region (below the velocity of 0.75) and a main flow is surrounded the vortical flow. The center of vortical flow is the position having a minimum kinetic energy. A reverse flow region presented by gray color in Fig. 13(a) is also observed near the casing wall. On the other hand, the high velocity fluctuation is observed in the interference region between the tip leakage vortex and the main flow as well as in the vortex core as shown in Fig. 13(b).

Fig. 14 shows the spectral distributions of the velocity fluctuation at the positions selected near the rotor tip on the quasi-orthogonal plane of Fig. 13 for the fan having the 2 mm TC operating in the design condition. The spectra are obtained by a FFT analyzer, which averages each value 64 times at a measuring position. In the present study, the spectra are measured at 49 grid points for one operating condition. Among them, the spectra at 12 positions shown by $\times$ symbols in Fig. 13(b) are selected at the three radial positions of 0.98(RI), 0.96(RII) and 0.9(RIII) span. Four positions (RI-E, RI-F, RII-E, and RII-F in Fig. 13(b)) of them exist in the reverse flow region. It is found that spectral peaks near the 400 and 500 Hz are found in the reverse flow region, although

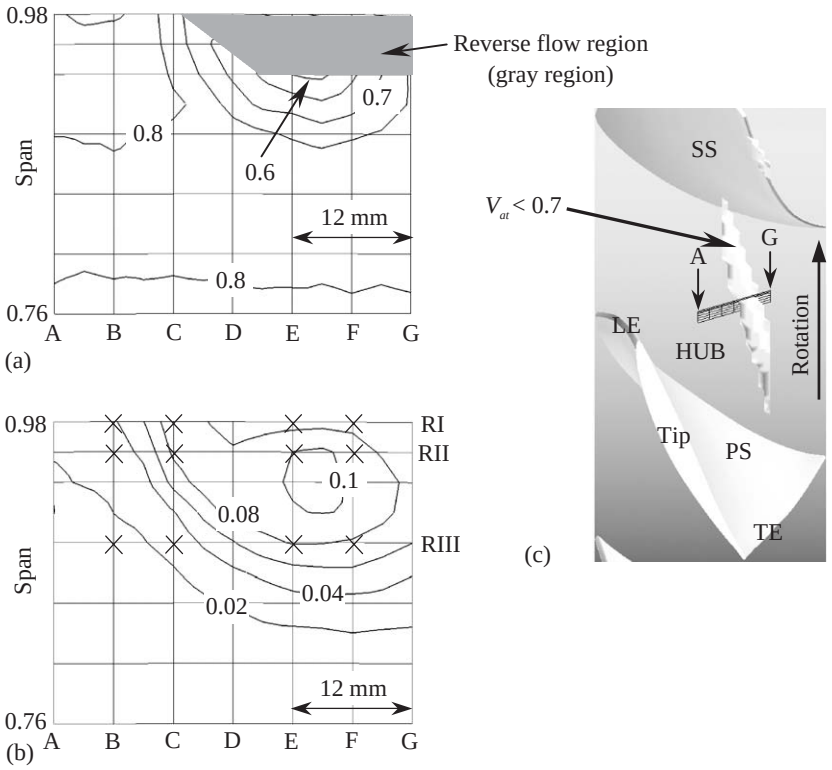

Fig. 13. Contour of relative velocity and velocity fluctuation on the quasi-orthogonal plane to the tip leakage vortex ($TC = 2$ mm, $\Phi = 0.39$): (a) Contour of relative velocity, V_{at} (interval of contour lines = 0.05), (b) contour of velocity fluctuation, V_f (interval of contour lines = 0.02), and (c) measuring position.

the peak of the velocity fluctuation spectrum is not clear upstream and downstream of the vortical flow. Kameier and Neise [6] also reported that TC noise of an axial turbomachine is caused by reverse flow in relation to the rotating flow instability near the rotor tip.

3.4. *Spectral peaks of fluctuating velocity at an off-design operating condition*

It has been reported by many researchers that undesired phenomena on the fan performance and noise increase due to a rotating instability and stall in the axial fans operating in a low flow condition. In the present study, the vortical flow structure and the spectral characteristics of the fluctuating velocity in the blade passage are investigated in the axial flow fans having the 2 and the 4.5 mm TCs operating at the off-design condition of $\Phi = 0.31$.

Fig. 15 shows the contour of relative velocity and velocity fluctuation on the three quasi-orthogonal planes to the axis of the tip leakage vortex of the axial flow fan having the 2 mm TC operating at the off-design condition. The positions of the measuring planes (I, II and III) in the blade passage are shown in Fig. 15(b), which is a perspective view from casing. The low relative velocity region spreads out to 85 per cent span from the casing according to decrease of flow rate

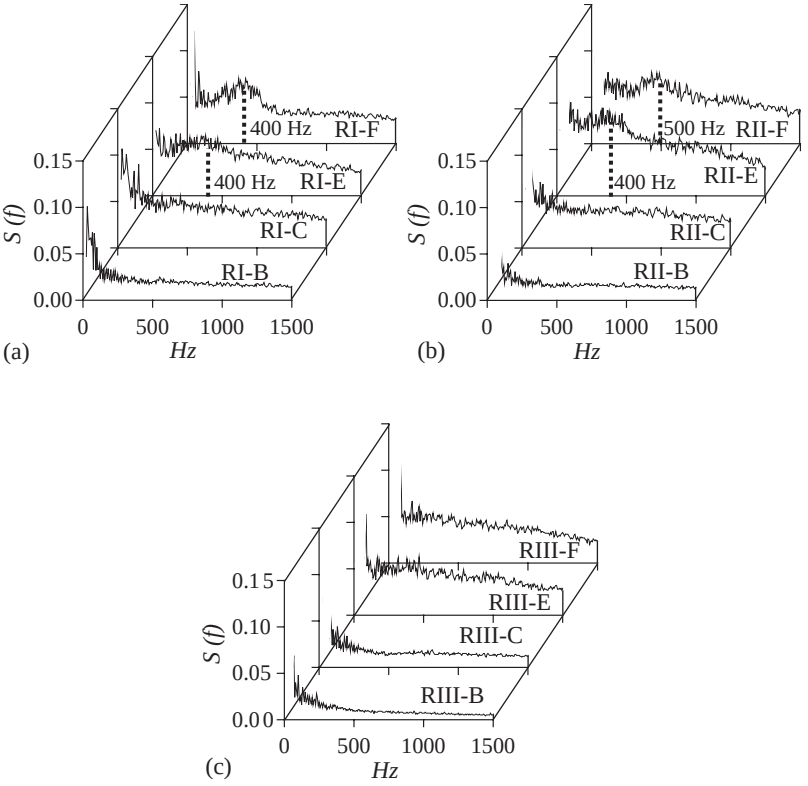

Fig. 14. Spectrum distributions of velocity fluctuation on the quasi-orthogonal plane of Fig. 13 ($TC = 2$ mm, $\Phi = 0.39$): (a) 0.98 span (RI), (b) 0.96 span (RII), and (c) 0.90 span (RIII).

as shown in Figs. 13(c) and 15(b). The larger velocity region is caused by as a result of the increase of the blockage of the vortical flow and the loss production in the blade passage. From the distributions of the relative velocity on the three planes as shown in Figs. 15(a), (c) and (e), vortical flow pattern is again clearly observed. High velocity fluctuation is observed in the interference region between the tip leakage vortex and the main flow as shown in Figs. 15(d) and (f). It is also noted that the low velocity region is expanded out as the vortical flow is moved to the streamwise direction. The reverse flow region is also increased as the flow rate is decreased because of the expansion of the vortical flow due to its large movement in time.

Fig. 16 shows the spectra of the velocity fluctuation at the positions selected on planes II and III of Fig. 15(b). At each plane, the spectra at 12 positions presented by $\times$ symbols in Figs. 15(d) and (f) are selected at the three radial positions of 0.98(RI), 0.96(RII) and 0.9(RIII) span. Spectral peaks near the 250 Hz are mainly observed in the reverse flow region like in the design operating condition. It should be noted that the intensity of the high velocity fluctuation is increased about 40 per cent compared to that at the design operating condition. Needless to say, the higher intensity of the velocity fluctuation is the important source of the broadband noise increase as described in the previous section.

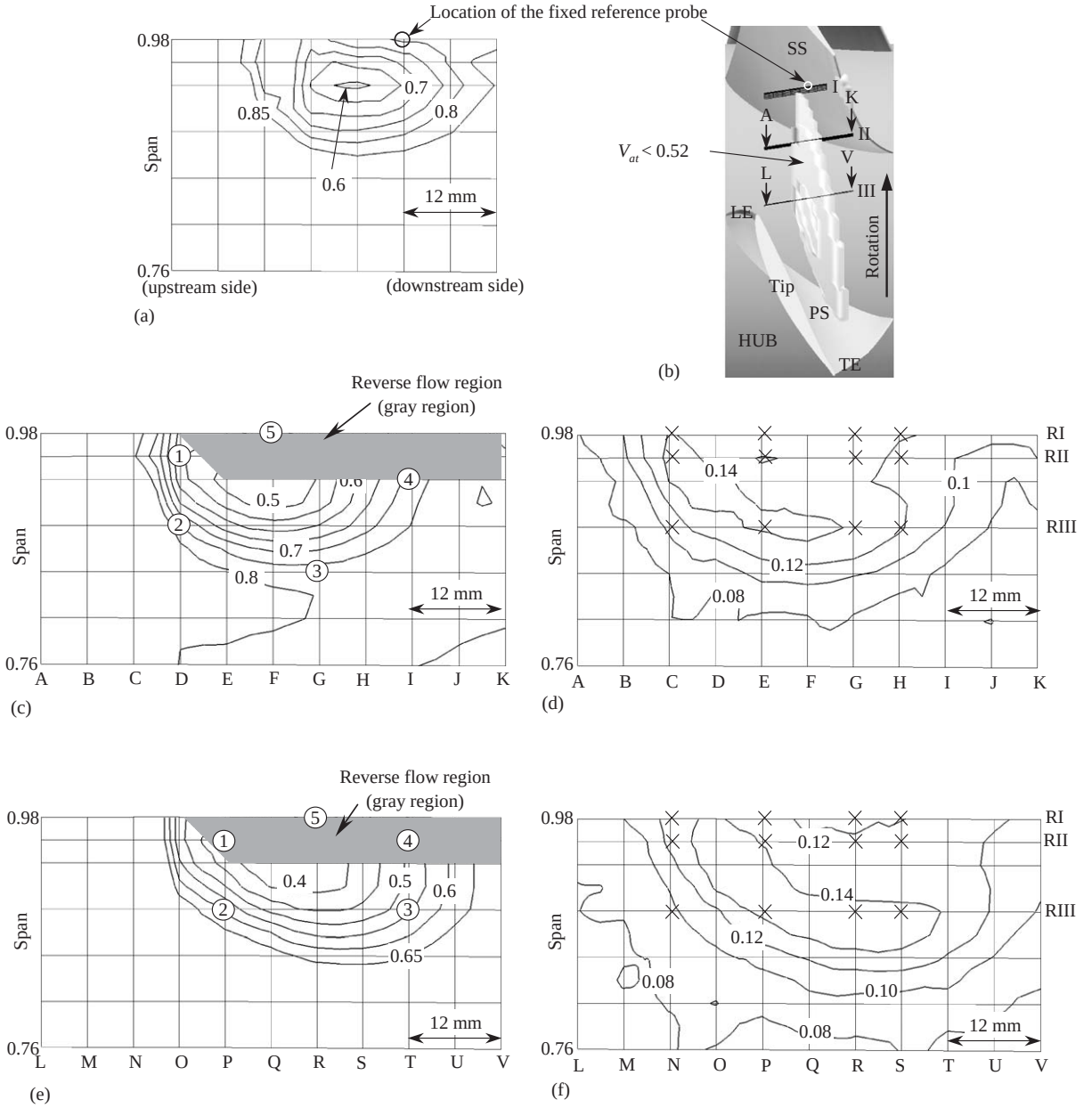

Fig. 15. Contour of relative velocity and velocity fluctuation on the quasi-orthogonal plane to the tip leakage vortex ($TC = 2$ mm, $\Phi = 0.31$): (a) contour of relative velocity on plane I (interval of contour lines = 0.05), (b) measuring position, (c) contour of relative velocity on plane II (interval of contour lines = 0.05), (d) contour of velocity fluctuation on plane II (interval of contour lines = 0.02), (e) contour of relative velocity on plane III (interval of contour lines = 0.05), and (f) contour of velocity fluctuation on plane III(interval of contour lines = 0.02).

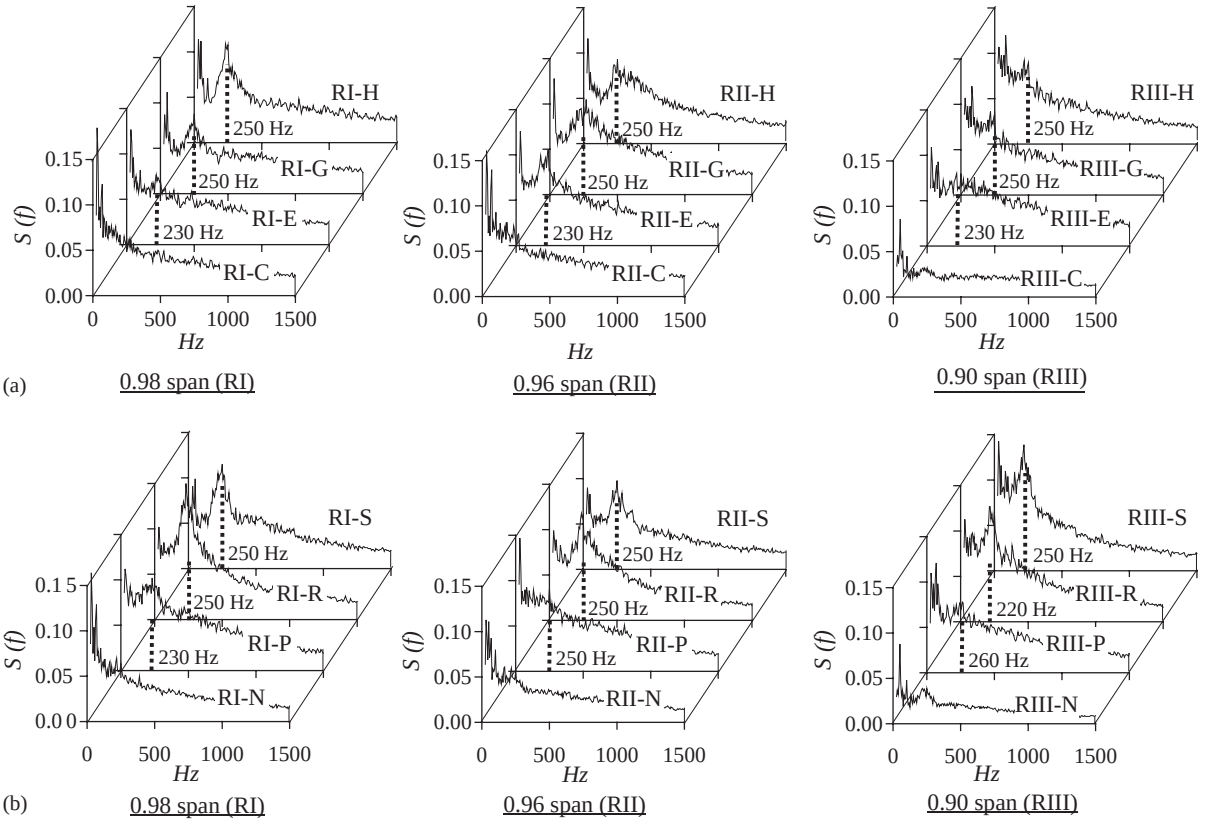

Fig. 16. Spectrum distributions of velocity fluctuation on the quasi-orthogonal plane of Fig. 15 ($TC = 2$ mm, $\Phi = 0.31$): (a) plane II in Fig. 15 and (b) plane III in Fig. 15.

Fig. 17 shows the contour of relative velocity and the velocity fluctuation for the 4.5 mm TC at the off-design operating condition. The positions of the measuring planes in the blade passage are shown in Fig. 17(b), which are presented in the same manner as shown in Fig. 15. As shown in Fig. 17, the vortical flow is expanded to 0.75 span from the casing. That is, the vortical flow is increased about 12 per cent in the radial direction compared to that for the 2 mm TC due to the larger TC flow. High velocity fluctuation on planes II and III is observed at the interference region between the tip leakage vortex and the main flow. The intensity of the velocity fluctuation is also increased as the TC is enlarged.

Fig. 18 shows the spectral distributions of the velocity fluctuation at the positions selected on planes II and III of Fig. 17(b). Spectral peaks near the 160 Hz are observed at all measuring position including the reverse flow region. The intensity of a spectral density $S(f)$ as shown in Fig. 18 of the fan having the 4.5 mm TC is about twice compared to that for the 2 mm TC. This means that the higher spectral peak at 160 Hz is more effective on the increase of a noise level. It is noted that the discrete frequency at the off-design operating condition have a lower value compared to that at the design condition because of the larger expansion of the vortical flow.

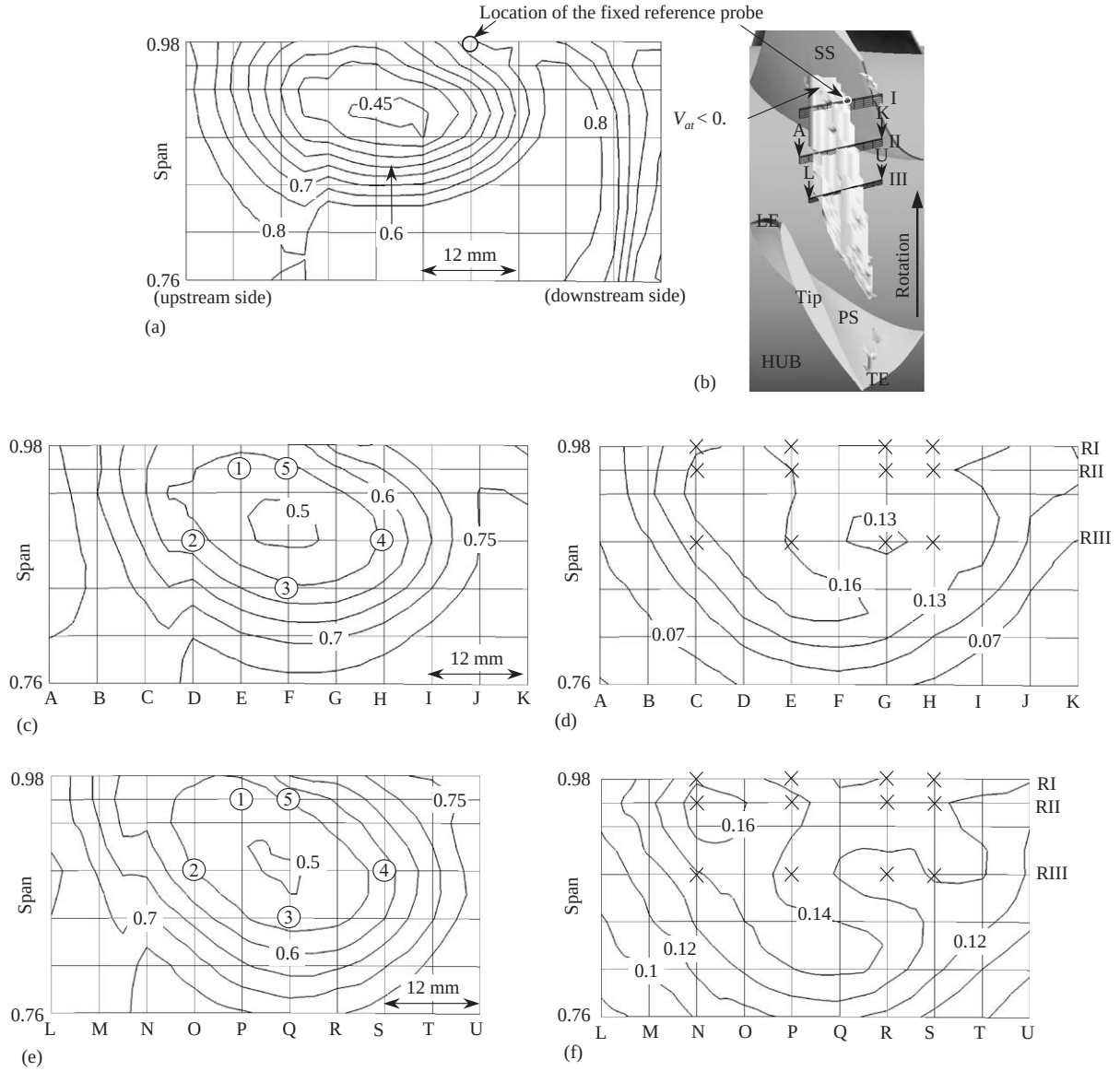

Fig. 17. Contour of relative velocity and velocity fluctuation on the quasi-orthogonal plane to the tip leakage vortex ($TC = 4.5$ mm, $\Phi = 0.31$): (a) contour of relative velocity on plane I (interval of contour lines = 0.05), (b) measuring position, (c) contour of relative velocity on plane II (interval of contour lines = 0.05), (d) contour of velocity fluctuation on plane II (interval of contour lines = 0.03), (e) contour of relative velocity on plane III (interval of contour lines = 0.05), and (f) contour of velocity fluctuation on plane III (interval of contour lines = 0.02).

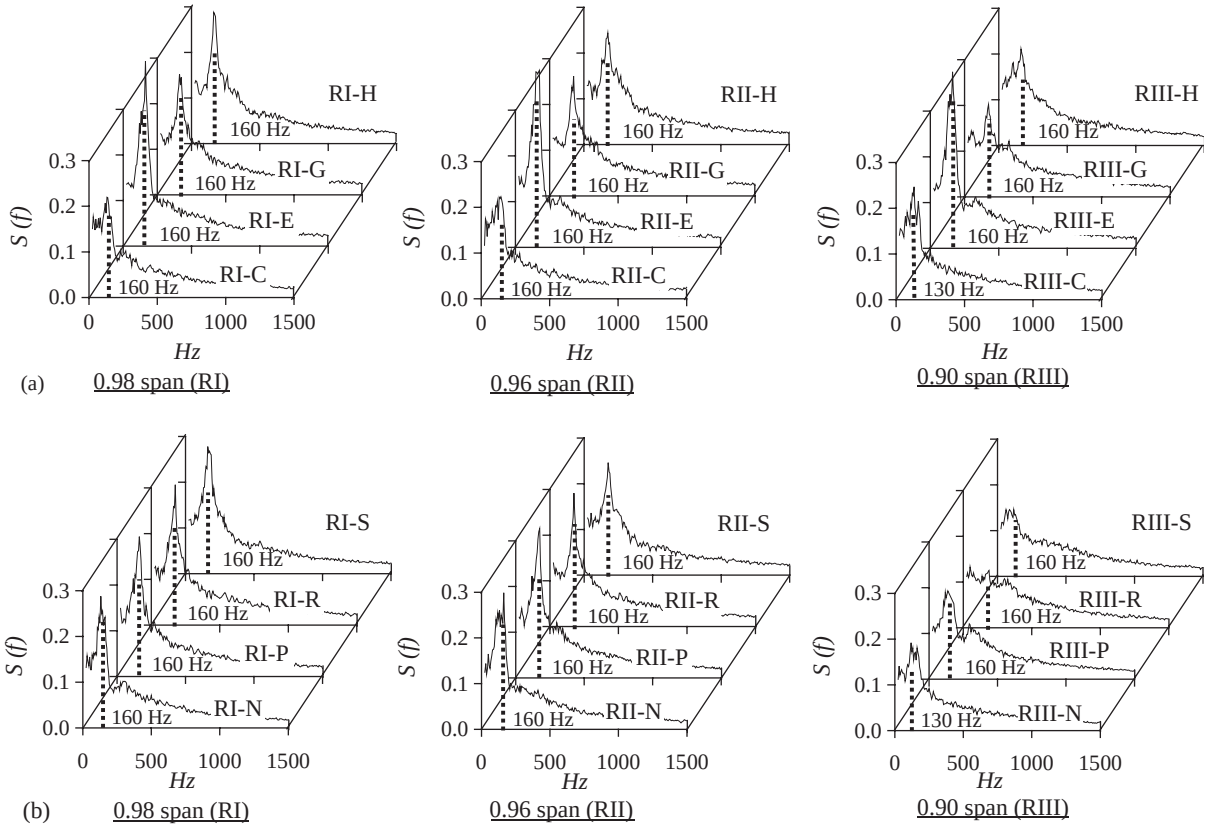

Fig. 18. Spectrum distributions of velocity fluctuation on the quasi-orthogonal plane of Fig. 17 ($TC = 4.5$ mm, $\Phi = 0.31$): (a) plane II in Fig. 17 and (b) plane III in Fig. 17.

3.5. *Analysis of cross-correlation in the leakage flow and retarded time at an off-design operating condition*

As described in the previous sections, the high velocity fluctuation and the spectral peaks due to the fluctuating velocity are observed near the vortical flow region. The frequency having a spectral peak in the vortical flow has a different value according to the TC and the flow rate in the axial flow fans. To understand the generation mechanism of the frequency having a spectral peak, it is effective to analyze the cross-correlation of the real-valued velocities between one reference position and target ones selected in the vortical flow. That is, the unsteady nature of the spectra of the real-time velocities measured by two hot-wire sensors in the vortical flow region is investigated by using cross-correlation coefficient and retarded time of the two fluctuating velocities.

Fig. 19 shows one example of the cross-correlation (C-C) coefficient and the retarded time for two real-valued velocities measured by the two hot-wire sensors: one is positioned at the fixed reference point marked by ○ as shown on plane I of the Figs. 15(a) and (b) and the other is at ④ on plane II of the Fig. 15(c). Both selected positions are located inside the vortical flow. Two fluctuating velocities shown in Fig. 19(a) are obtained by filtering the frequency between 240 and

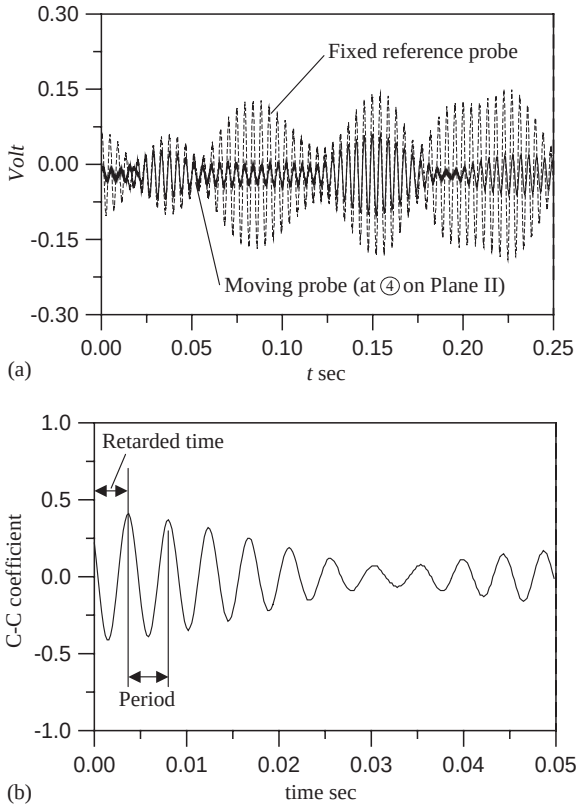

Fig. 19. Example of cross-correlation (C-C) coefficient and retarded time for two real-valued signals ($TC = 2$ mm, $\Phi = 0.31$): (a) fluctuating signals of two real-valued velocities and (b) cross-correlation coefficient.

260 Hz to the real-valued velocities measured by two hot-wire sensors. The band-pass filter selected has the band of 10 Hz to the peak frequency of 250 Hz as shown in Fig. 16. In the present measurement, the sampling frequency of the real-valued signals is 5120 Hz, which corresponds 20 times the frequency of 250 Hz. A measuring time of the two fluctuating velocities is 0.6 s (about 80 fan revolutions). It is notice that the 250 Hz velocity component is not steady because the amplitude fluctuates considerably.

The cross-correlation coefficient of the two fluctuating velocities are shown in Fig. 19(b). In the figure, the retarded time is determined by the delayed time of the first peak of the cross-correlation coefficient. The period of the two fluctuating velocities is the delayed time between the first peak of the cross-correlation coefficient and the second one as shown in Fig. 19(b).

Figs. 20(a) and (b) respectively show the distribution of the cross-correlation at 5 positions on planes II and III for the 2 mm TC at $\Phi = 0.31$. The five positions are distributed in the vortical flow region as shown in Figs. 15(c) and (e). The coefficient shows a high value over 0.7 at almost positions. This is the evidence that the real-valued velocities measured at the fixed reference position and the corresponded positions on planes II and III have similar spectra. Throughout the value of the coefficient on planes II and III, it can be concluded that the velocity fluctuation in the

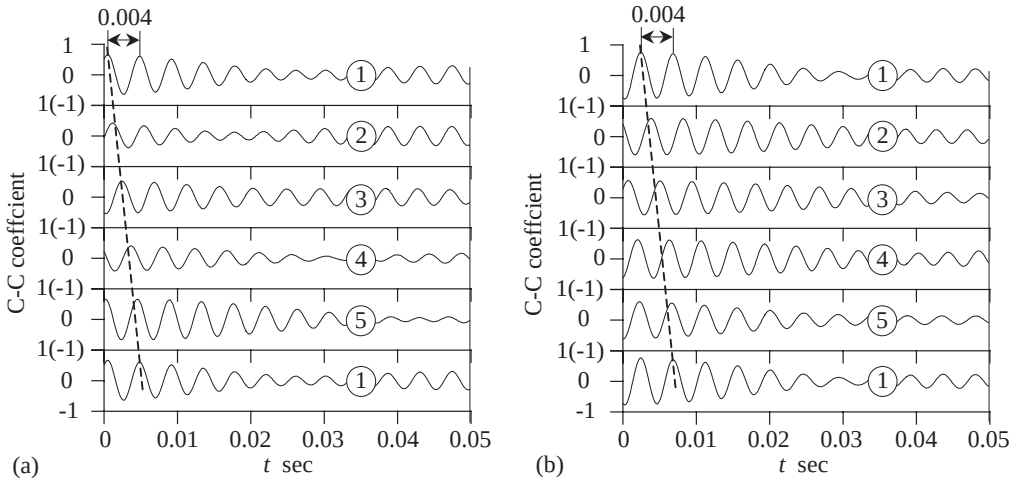

Fig. 20. Distribution of cross-correlation (C-C) coefficient on planes II and III ($TC = 2$ mm, $\Phi = 0.31$): (a) plane II and (b) plane III.

vortical flow has a close relation to that of upstream. This also implies that the vortical flow is the tip leakage flow.

On the other hand, a counter-clockwise vortical flow is clearly observed through the retarded time presented by a dashed line in Fig. 20. The period of the fluctuating velocities is 0.004 s (250 Hz) on the planes II and III, which corresponds the frequency having spectral peak as shown in Fig. 16. That is, the frequency of 250 Hz is the result of a period for one revolution of the vortical flow.

Fig. 21 shows the distribution of the cross-correlation at 5 positions on planes II and III for the 4.5 mm TC at $\Phi = 0.31$, which is presented in the same manner as Fig. 20. The five positions are in the vortical flow region as shown in Figs. 17(c) and (e). The coefficient having a high value over 0.7 is also shown at almost positions. A counter-clockwise vortical flow from the distribution of the retarded time presented by dashed line is also observed, which has the period of about 0.006 s (167 Hz) in Fig. 21. The period for one revolution of the vortical flow has a fairly good agreement to the frequency having the spectral peak in Fig. 18.

3.6. Tip clearance noise caused by the unsteady vortical flow

As described in the previous sections, the peak frequencies in the vortical flow are closely related to the behavior of the low velocity due to the tip leakage vortex. It is well known that the tip leakage vortex has a three-dimensional and unsteady nature in axial flow fans. As shown in Fig. 19(a), the unsteady characteristic of vortical flow is observed from the fluctuating velocity filtered between 240 and 260 Hz, and the fluctuating velocity is changed in time with amplification and attenuation of its amplitude repeatedly as already pointed out.

To describe the generation mechanism of the peak frequency in the vortical flow, the authors propose a spiral pattern of the source of velocity fluctuation as shown in Fig. 22: that is, a small lump of low velocity is moved streamwise direction along a spiral-type vortical structure. For example, the peak frequency of 250 Hz in Fig. 16, which is measured at fixed positions in the

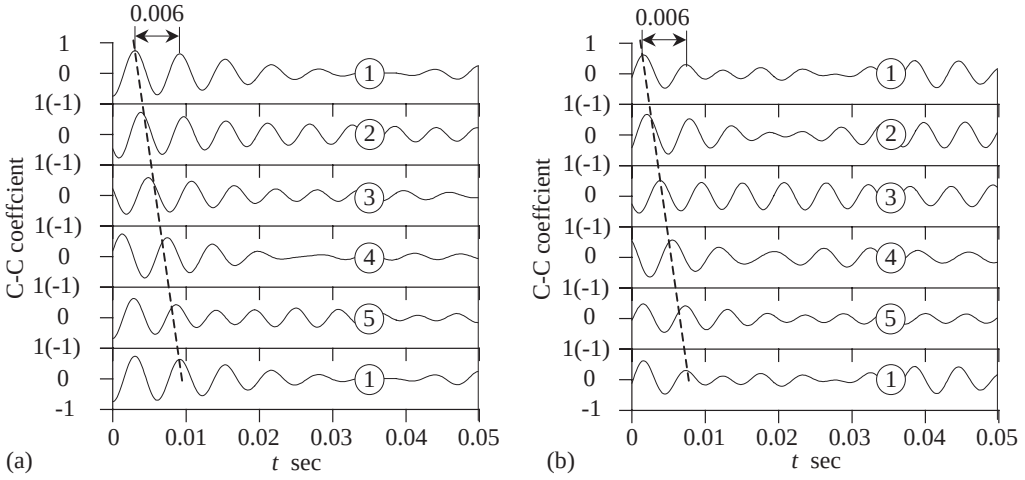

Fig. 21. Distribution of cross-correlation (C-C) coefficient on planes II and III ($TC = 4.5$ mm, $\Phi = 0.31$): (a) plane II and (b) plane III.

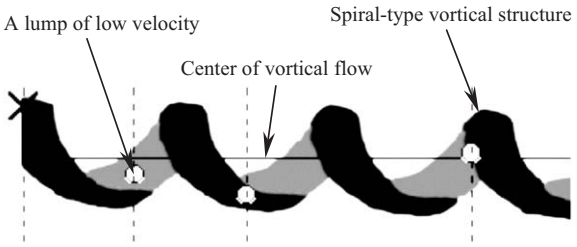

Fig. 22. Spiral pattern of velocity fluctuation.

relative frame of reference rotating with the rotor, is generated because the lump of low velocity moving downstream with rotation takes 0.004 s for one rotation along the spiral-type vortical structure. Of course, the lump of low velocity is in the low velocity region generated by the tip leakage vortex. The peak frequency of 250 Hz at the rotational speed of 1000 r.p.m. is close to that of the noise as shown by a dotted line for $\Phi = 0.31$ in Fig. 9.

Fig. 23 shows the spectrum of velocity fluctuation according to the rotational speed of the fan rotor having 2 mm TC at $\Phi = 0.31$. The peak frequency is proportionally increased by the increase of the rotational speed of the fan rotor.

Fig. 24 shows the relation between the peak frequency and the rotational speed of the fan rotor with the flow rate. The peak frequency also increases with the flow rate at the constant rotational speed of the fan rotor. This implies that the noise due to the peak frequency can be an important noise source when the fans are rotated with a high rotational speed.

Finally, the spectra of noise in the axial fans having two different TCs operating at the design ($\Phi = 0.39$) and the off-design condition ($\Phi = 0.31$) are shown in Figs. 25(a) and (b). In the figure, dashed vertical lines indicate the harmonic of blade passing frequency. At the design operating condition, two peak frequencies of 400 and 500 Hz indicated by open circle in Fig. 25(a)

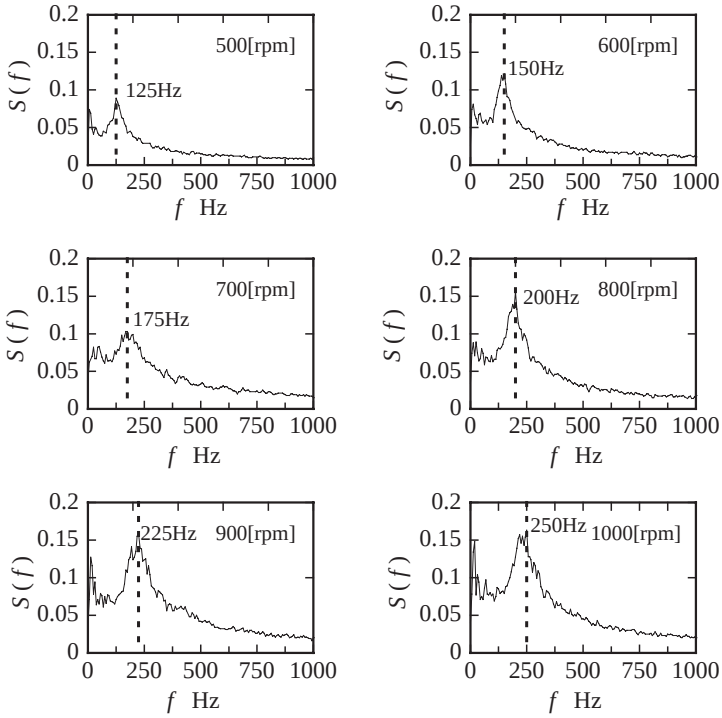

Fig. 23. Spectrum of velocity fluctuation according to the rotational speed of fan rotor ($TC = 2\,\text{mm}$, $\Phi = 0.31$).

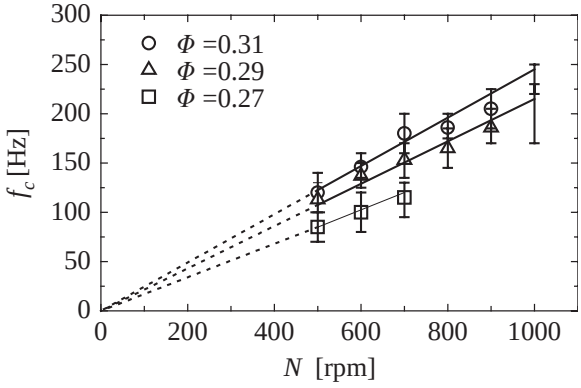

Fig. 24. Peak frequency of velocity fluctuation according to the rotational speed of fan rotor ($TC = 2\,\text{mm}$).

correspond the frequencies having spectral peak obtained by fluctuating velocity in the vortical flow as shown in Fig. 14. The peak frequencies of 250 and 160 Hz at $\Phi = 0.31$ as shown in Figs. 16 and 18 are also clearly observed in the noise spectrum in Fig. 25(b) for the two TCs. The discrete frequency noise due to spectral peak as well as the broadband noise are increased as the TC is enlarged at the same flow condition, which are caused by larger vortical flow due to the increased

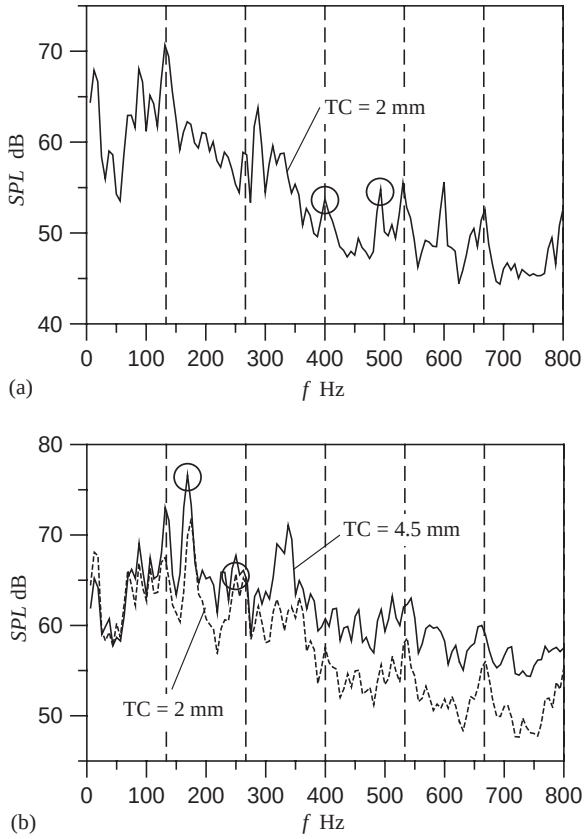

Fig. 25. Spectra of noise: (a) design operating condition ($\Phi = 0.39$) and (b) off-design operating condition ($\Phi = 0.31$).

clearance flow. It is noted that the noise due to TC in the axial flow fans has effect on the low frequency band [5].

4. Conclusions

The noise due to TC in axial flow fans having two different TCs is investigated by experimental analysis using two rotating hot-wire sensors at a design and off-design operating conditions. The results are summarized as follows:

1. Noise increase due to TC at low flow rate conditions is mainly caused by high velocity fluctuation in a vortical flow and the interference between tip leakage vortex and adjacent pressure surface as well as the casing surface. The intensity of velocity fluctuation is increased by enlarging the TC and decreasing the flow rate.
2. The peak frequencies in a vortical flow are mainly observed below at four harmonic blade passing frequency. The peak frequencies of the velocity fluctuation at off-design operating conditions are generated in the vortical flow region as well as in the reverse flow region while

the frequencies at the design operating condition are mainly observed in the reverse flow region.

3. The peak frequency of the velocity fluctuation is proportionally increased by the increase of the rotational speed of the fan rotor. The frequency is also increased with the increase of the flow rate at the constant rotational speed of the fan rotor. This implies that the noise due to the peak frequency can be and important noise source when the fans are rotated with a high rotational speed.
4. The discrete frequency at off-design operating conditions has a lower value compared to that at a design condition because of the larger expansion of the vortical flow. The larger vortical flow, which results in large blockage in the blade passage, generates a high velocity fluctuation at the interference region between the vortical flow and main flow.
5. The unsteady nature of the spectra of the real-time velocities measured by two hot-wire sensors in the vortical flow region is investigated by using cross-correlation coefficient and retarded time of the two fluctuating velocities. The period for one revolution of the vortical flow has a fairly good agreement to the frequency having the spectral peak.
6. To describe the generation mechanism of the peak frequency in the vortical flow, the authors propose a spiral pattern of velocity fluctuation: that is, a small lump of low velocity is moved streamwise direction along a spiral-type vortical structure. It is found that the fluctuating velocity presenting a spectral peak is randomly changed in time with amplification and attenuation of its amplitude repeatedly.
7. The peak frequency obtained by the rotating hot-wire sensor in the vortical flow corresponds well to the one of the noise spectrum measured by microphone. This means that the noise due to TC flow is generated by the discrete frequency noise due to spectral peak as well as the broadband noise due to velocity fluctuation.

Acknowledgements

The authors are grateful to Mr. N. Ogata and Mr. D. Sato for their assistance in this experiment.

References

[1] M. Inoue, M. Kuroumaru, Structure of tip clearance flow in an isolated axial compressor rotor, *American Society of Mechanical Engineers, Journal of Turbomachinery* 111 (3) (1989) 250–256.

[2] J.A. Storer, N.A. Cumpsty, Tip leakage flow in axial compressors, *American Society of Mechanical Engineers, Journal of Turbomachinery* 113 (1991) 252–259.

[3] B. Lakshminarayana, M. Zaccaria, B. Marathe, The structure of tip clearance flow in axial flow compressors, *American Society of Mechanical Engineers, Journal of Turbomachinery* 117 (1995) 336–347.

[4] R.E. Longhouse, Control of tip-vortex noise of axial flow fans by rotating shrouds, *Journal of Sound and Vibration* 58 (1978) 201–214.

[5] T. Fukano, Y. Takamatsu, Y. Kodama, The effects of tip clearance on the noise of low pressure axial and mixed flow fans, *Journal of Sound and Vibration* 105 (1986) 291–308.

[6] F. Kameier, W. Neise, Experimental study of tip clearance losses and noise in axial turbomachines and their reduction, *American Society of Mechanical Engineers, Journal of Turbomachinery* 119 (1997) 460–471.

[7] T. Fukano, H. Saruwatari, H. Hayashi, H. Isobe, M. Fukuhara, Periodic velocity fluctuation in the near wake of a rotating flat-plate blade and their role in the generation of broadband noise, *Journal of Sound and Vibration* 181 (1995) 53–70.

[8] C.-M. Jang, N. Ogata, M. Furukawa, T. Fukano, Characteristics of three-dimensional flow field and velocity fluctuation near the rotor tip in an axial flow fan, *Transactions of the Japan Society of Mechanical Engineers* 68 (673) (2002) 2460–2466 (in Japanese).

[9] N. Curle, The influence of solid boundaries upon aerodynamic sound, *Proceedings of the Royal Society A* 231 (1955) 505–514.